scientific reports

Check for updates

OPEN

Identification and characterization of a dsRNA-degrading nuclease CmdsRNase2 influencing RNAi efficiency in the rice leaffolder *Cnaphalocrocis medinalis*

Xin Wang[1,2], Juan Du[1,2], Shangwei Li[1,2]✉, Jiajing Li[1,2] & Renming Zha[2]✉

The rice leaffolder *Cnaphalocrocis medinalis* is one of the most important pests of rice. Double-stranded RNA-degrading enzyme (dsRNase) is one of key factors affecting the stability of dsRNA in insects, thus restricting the application of RNA interference (RNAi) technology in pest control. In this study, a *dsRNase* gene from *C. medinalis*, designated *CmdsRNase2*, was cloned by using reverse transcription-polymerase chain reaction (RT-PCR). The open reading frame (ORF) of *CmdsRNase2* is 1,335 bp in length, encoding 444 amino acids. The CmdsRNase2 protein contains a signal peptide and an Endounuclease_NS domain that includes six active sites, one Mg^{2+} binding site, and three substrate binding sites. Homology comparison showed that CmdsRNase2 was most closely related to dsRNase2 from *Ostrinia nubilalis*, with 66.96% similarity. Spatiotemporal expression pattern analyses indicated that *CmdsRNase2* was expressed throughout developmental stages with the highest expression level in the fifth-instar larvae and all seven tissues tested in adults with the highest level in the hemolymph. On the third day after RNA interference (RNAi), silencing *CmCHS* (*C. medinalis chitin synthase*) alone had a RNAi efficiency of 56.84%, while co-sliencing both *CmCHS* and *CmdsRNase2* caused a RNAi efficiency of 83.44%, an increase of 26.60%. The results showed that the efficiency of RNAi in *C. medinalis* was greatly improved by simultaneously interfering with expressions of both *CmCHS* and *CmdsRNase2*. This study is very helpful for understanding the mechanism of dsRNase involved in the RNAi process and for eco-friendly pest control by using RNAi strategies.

Keywords *Cnaphalocrocis medinalis*, DsRNA-degrading nuclease (dsRNase), RNA interference (RNAi), RNAi efficiency

RNA interference (RNAi) refers to the highly conserved phenomenon of high-efficiency and specific degradation of homologous messenger RNA (mRNA) induced by double-stranded RNA (dsRNA) during evolution. The essence of RNAi is post-transcriptional gene silencing (PTGS). The transcription of the silenced gene still proceeds normally, but the transcribed mRNA undergoes sequence-specific degradation in the cytoplasm, resulting in the gene not being expressed normally into protein. The phenomenon of PTGS was first discovered in plants, but the real cause of gene silencing was not elucidated until 1998, when Fire et al. first reported the phenomenon of RNAi mediated by dsRNA in *Caenorhabditis elegans*. Exogenous dsRNA can silence homologous endogenous mRNA in organisms, which is called RNAi[1]. The use of RNAi technology to control pests is one of the hotspots of current scientific research. In entomological research, it has been found that the production of RNAi can be induced in a variety of insects by injecting, feeding, and introducing dsRNA or small interfering RNA (siRNA)[2]. RNAi is a well-established reverse genetics approach for exploring gene function in insects. Although RNAi is an indispensable research tool in many insect species, RNAi responses are highly variable and some insects have limited RNAi capabilities[3–5]. Variations in RNAi responses in different insects have been attributed to a wide range of factors, including changes in the stability of dsRNA across insects, differences in cellular uptake of dsRNA molecules, differences in intracellular distribution and processing of dsRNA, and

[1]Guizhou Key Laboratory of Agricultural Biosecurity, Institute of Entomology, Guizhou University, Guiyang 550025, Guizhou, China. [2]College of Agriculture, Guizhou University, Guiyang 550025, Guizhou, China. ✉email: swlii@163.com; zrm1966@163.com

systemic differential distribution of effector molecules. In these factors, the most widely studied is the stability of dsRNA when delivered to insects. In many insect species, RNA-mediated knockdown of gene transcripts can be achieved by direct injection of dsRNA into the blood cavity, but because this delivery method is technically challenging and time-consuming, many researchers have sought to develop feed formula for higher throughput dsRNA applications. Although many successful dsRNA feeding experiments have been reported, a growing body of research has observed that dsRNases in insects can greatly reduce the efficacy of RNAi[6]. RNAi does not act the same across all insects, thus limiting the ability of RNAi to control certain insects, especially lepidopterans[7].

DsRNA-degrading nucleases (dsRNases) belong to the DNA/RNA non-specific endonuclease (NUC), a family of bacterial and eukaryotic endonucleases that act on both DNA and RNA and cleave double-stranded (ds) and single-stranded (ss) nucleic acids[8,9]. NUCs require a divalent ion such as magnesium to degrade dsDNA, ssDNA, and dsRNA[10,11]. There are two types of NUCs in insects, namely endonuclease G (EndoG) and dsRNase. EndoG is a ubiquitous nuclease that moves into the nucleus to help degrade DNA during apoptosis[12]. However, dsRNases have been shown to degrade dsRNA, thus reducing the efficiency of RNAi[9]. The degradation of exogenous dsRNA is one of the key factors restricting the application of RNAi technology in pest control[13,14]. In 1965, Mukai purified a Mg^{2+}-activated alkaline endonuclease from the digestive juice of *Bombyx mori* larvae, and this enzyme hydrolysed DNA and RNA[15]. Avian cells expressed a novel dsRNase, but its role was unclear[16]. Subsequent studies showed that dsRNA could also induce dsRNase in mammalian cells[17]. In 2012, a study by Liu et al.. demonstrated that BmdsRNase from the digestive juice of *B. mori* could degrade dsRNA and this activity interfered with the RNAi response[18]. Surprisingly, *dsRNase* gene sequences only from insects and crustaceans were found in publicly available eukaryotic nucleic acid sequence databases. Four different dsRNase sequences were retrieved in the transcriptome database of *Schistocerca gregaria* and results of RNAi experiments on the desert locust showed that dsRNase was an important contribution to low RNAi efficiency[19]. Therefore, many scholars focused on the study of the effect of dsRNases on the RNAi efficiency in insects. Previous studies indicated that degradation of dsRNA was a major factor limiting the RNAi efficiency in lepidopterans[20–22].

Rice leaffolder *Cnaphalocrocis medinalis* (Lepidoptera: Pyralidae) is a migratory pest of rice, and can also be found on other graminaceous plants such as maize and wheat[23–25]. *C. medinalis* larvae affect photosynthesis by feeding on the leaf epidermis and mesophyll, thereby reducing rice yield[26]. As one of the most destructive and major rice pests in Asia, some pesticides have been used to deal with this pest. However, due to concerns about pesticide resistance, residues, and environmental hazard, it is urgent to find a green management strategy to control this pest[27,28]. Although RNAi is a promising technology for controlling pests, the RNAi efficiency in *C. medinalis* is generally low; therefore, there are some limitations in using RNAi to control this pest. In order to apply the RNAi technology to the biological control of *C. medinalis*, it is of great importance to study the action process of RNAi and factors affecting the RNAi efficiency.

Materials and methods

Insect rearing

C. medinalis was collected from a rice field in Guiyang, Guizhou, China, and maintained in an insectary of the Institute of Entomology, Guizhou University, at 26 °C ± 1 °C and 75% ± 5% relative humidity under a 14:10 h light: dark photoperiod. Samples were collected and then stored in RNAlater (Qiagen, Duesseldorf, Germany) at −20 °C until use. These samples included eggs, first- to fifth-instar larvae, pupae, adults, and adult tissues (the head, integument, fat body, testis, ovary, midgut, and hemolymph).

RNA extraction and cloning of the *CmdsRNase2* cDNA

An HP Total RNA Kit (Omega Bio-Tek Inc., Norcross, GA, USA) was used to extract total RNA from different developmental stages and from various different adult tissues. The hemolymph was extracted by using a double-tube method described by Li et al.[29] and Mo et al.[30]. The purity and concentration of RNA were determined using a NanoDrop 2000 spectrophotometer (Thermo Fisher Scientific, Waltham, MA, USA), and the quality of RNA was detected by using 1% agarose gel electrophoresis. RNA was used as a template to synthesize cDNA with a RevertAid First Strand cDNA Synthesis Kit (Thermo Fisher Scientific, Waltham, MA, USA). The synthesized cDNA was stored at −20 °C. Based on the sequence information from the *C. medinalis* transcriptome, primers were designed with Primer Premier 6.0 (PREMIER Biosoft, Palo Alto, CA, USA) (Table 2) and reverse transcription-polymerase chain reaction (RT-PCR) was carried out with 2× PCR Master Mix. Reaction parameters were as follows: 95 °C for 2 min; 35 cycles of 95 °C for 30 s, 54 °C for 30 s, and 72 °C for 1 min; and a final extension of 72 °C for 10 min. PCR products were detected by using 1% agarose gel electrophoresis and then recovered by employing a SanPrep Column DNA Gel Extraction Kit (Sangon Biotech, Shanghai, China). The purified DNA was then cloned into a pMD18-T vector and transformed into *E. coli* Top10 competent cells. The cells were plated on LB agar plates with ampicillin and incubated at 37 °C overnight. Recombinant colonies were picked and inoculated into 5 mL of LB medium, and incubated at 37 °C overnight. Subsequently, 1 µl of each bacterial culture was added into a 20 µl of system to perform colony PCR using both dsRNases-F and dsRNases-R primers. Positive clones contained inserted DNA were sent to Sangon Biotech (Shanghai, China) for sequencing.

Bioinformatics analyses

We used the ORFfinder (https://www.ncbi.nlm.nih.gov/orffinder) to search the open reading frame (ORF) of *CmdsRNase2*. The Expasy ProtParam platform (https://web.expasy.org/protparam) was used to predict the molecular weight and isoelectric point (pI) of the CmdsRNase2 zymoprotein. The signal peptide was predicted with SignalP-6.0 (https://services.healthtech.dtu.dk/services/SignalP-6.0). Domains of this mature zymoprotein were analyzed with SMART (http://smart.embl.de) and CD-search (https://www.ncbi.nlm.nih.gov/Structure/cdd/wrpsb.cgi). Glycosylation sites were predicted by using NetOGlyc-4.0 (https://services.healthtech.dtu.dk/service.php?NetOGlyc-4.0) and NetNGlyc-1.0 (https://services.healthtech.dtu.dk/service.php?NetNGlyc-1.

0). Phosphorylation sites were predicted by employing NetPhos-3.1 (https://services.healthtech.dtu.dk/services/NetPhos-3.1/). Multiple sequence alignment was performed using Jalview (https://www.jalview.org) with the Muscle method. The phylogenetic tree was constructed by using the neighbor-joining (NJ) method in the MEGA 11 software with 1,000 runs. The three-dimensional structure of the mature CmdsRNase2 was predicted by employing SWISS-MODEL homologous modeling (https://swissmodel.expasy.org) and its molecular graphic was drawn using PyMOL 3.0 (Schrodinger, New York, NY, USA). The ConSurf Server (https://consurf.tau.ac.il) was used to analyze evolutionary conservation profile of CmdsRNase2.

Digital PCR

Absolute quantification of the *CmdsRNase2* mRNA was detected by using a Droplet Digital PCR (ddPCR) System (Bio-Rad, Hercules, CA, USA) at different developmental stages and in various tissues of *C. medinalis* adults. Briefly, 20 µl of PCR reaction solution and 70 µl of oil were partitioned into ~20,000 nanoliter-sized droplets with a QX200 Droplet Generator. Then, 40 µl of droplets from the cartridge were transferred into a 96-well PCR plate. After sealing the PCR plate with foil, PCR amplification was performed on a C1000 Touch Thermal Cycler with 96-deep well reaction module. The reaction system and thermal cycling conditions of ddPCR are listed in Table 1. After the PCR amplification was completed, droplets were analyzed on a QX200 Droplet Reader. PCR-positive and PCR-negative droplets were counted using QuantaSoft Software. Three replicates were performed for each sample.

RNA interference

Two online tools, i.e., siDirect (http://sidirect2.rnai.jp) and DSIR (http://biodev.extra.cea.fr/DSIR/DSIR.html) were used to design target fragments of *CmdsRNase2* and *CmCHS* (chitin synthase from *C. medinalis*), based on their ORFs. CmCHS is a key enzyme in the chitin synthesis pathway and is essential for the growth and development of this pest. *CmCHS* was used as a target gene to check how CmdsRNase2 affected the RNAi efficiency of *CmCHS* in *C. medinalis*. The *green fluorescent protein* (*GFP*) gene (GenBank accession number: CAA58789) from *Aequorea victoria* was used as the control. The cDNAs of these three genes were used as templates to amplify target fragments using dsRNase2-iF/dsRNase2-iR, CHS-iF/CHS-iR, and GFP-iF/GFP-iR primers, respectively. After purification, the PCR products were cloned into the pMD18-T vector (Takara Bio, Dalian, China) for sequencing. Clones containing the correct sequences were cultured for plasmid extraction. Plasmids were used as templates to amplify targets with dsRNase2-dsF/dsRNase2-dsR, CHS-dsF/CHS-dsR, and GFP-dsF/GFP-dsR primers, respectively. After purification, DNAs with high concentration (not less than 300 ng/µL) were obtained and then used as templates to synthesize ds*CmdsRNase2*, ds*CmCHS*, and ds*GFP* with a TranscriptAid T7 High Yield Transcription Kit (Thermo Fisher, Waltham, MA, USA). Briefly, 20-µL in vitro transcription system contained 2 µL of nuclease-free water, 4 µL of 5 × reaction buffer, 8 µL of ATP/CTP/GTP/UTP mix, 4 µL of DNA template, and 2 µL of enzyme mix. After being vortexed and briefly spun, this mixture was incubated at 37 °C for 6 h. The dsRNA was purified by using a GeneJET RNA Purification Kit (Thermo Fisher, Waltham, MA, USA) and then detected by both agarose gel electrophoresis and a NanoDrop 2000 spectrophotometer (Thermo Fisher, Waltham, MA, USA) to evaluate its integrity and quality. All primers used in this study are listed in Table 2.

Twenty third-instar *C. medinalis* larvae were used for the RNAi experiment in each group. RNAi experiments were set up into four groups: injections of ds*CmdsRNase2*, dsCm*CHS*, ds*CmdsRNase2* + ds*CmCHS*, and ds*GFP*. For each larva, 1.5 µg of dsRNAs were injected into the hemocoel through the eighth abdominal segment using a Nanoliter 2020 Injector (World Precision Instruments, Sarasota, FL, USA). The dsRNA-injected larvae were fed with fresh rice leaves inside glass tubes in an artificial climate chamber with normal rearing conditions. During this period, the rice leaves were replaced with fresh ones every 2 d. The phenotype and survival of larvae were observed every 24 h. The RNAi experiment was repeated three times in each group. Two larvae were collected from each group at 24, 48, 72, and 96 h post injection for ddPCR detection.

Data analysis

Data were expressed as means ± SD from three independent experiments. Multiple comparisons were performed using one-way analysis of variance (ANOVA) and the Duncan's multiple range test with SPSS 22.0 (SPSS Inc., Chicago, IL, USA). A *P*-value less than 0.05 was considered as statistical significance.

Component	Volume per reaction, µL	Final concentration	Cycling step	Temperature, °C	Time	Number of cycles	Remarks
2× QX200 ddPCR EvaGreen Supermix	10	1×	Enzyme activation	95	5 min	1	Ramp rate: 2 °C/s Lid temperature: 105 °C Sample volume: 40 µl
Forward primer (2 µM)	1	100 nM	Denaturation	95	30 s	40	
Reverse primer (2 µM)	1	100 nM	Annealing and extension	60	1 min	40	
DNA template	1	200 ng	Signal stabilization	4	5 min	1	
DNase-free water	7	—		90	5 min	1	
Total volume	20	—	Hold	4	Infinite	1	

Table 1. The reaction system and parameters of ddPCR.

Primer name	Primer sequence (5′→3′)	Primer usage
dsRNase2-F	ATGCGTTGTTTGGTGATATGGGC	RT-PCR
dsRNase2-R	TTATGTCAGAAGGCCATTAACTTTCC	
dsRNase2-dF	CCGTTCGTGCTTCAACACAATC	ddPCR
dsRNase2-dR	GAACAACATTCGCCTCGTGGAT	
CHS-dF	TGGAATACCTTCGCCAGTCATC	
CHS-dR	CCAGGAACACCAGGAGGCATT	
dsRNase2-iF	CGGTCATCTACACGGGAACAT	dsRNA synthesis
dsRNase2-iR	GTCAGAAGGCCATTAACTTTCC	
dsRNase2-dsF	taatacgactcactatagggCGGTCATCTACACGGGAACAT	
dsRNase2-dsR	taatacgactcactatagggGTCAGAAGGCCATTAACTTTCC	
CHS-iF	ACGAGGTTACACGAGAGG	
CHS-iR	CATCCAATGTTCCAATGTTCCT	
CHS-dsF	taatacgactcactatagggACGAGGTTACACGAGAGG	
CHS-dsR	taatacgactcactatagggCATCCAATGTTCCAATGTTCCT	
GFP-iF	GCCAACACTTGTCACTACTT	
GFP-iR	GGAGTATTTTGTTGATAATGGTCTG	
GFP-dsF	taatacgactcactatagggGCCAACACTTGTCACTACTT	
GFP-dsR	taatacgactcactatagggGGAGTATTTTGTTGATAATGGTCTG	

Table 2. Primers used for cloning and expression analysis of *CmdsRNase2* and for DsRNA synthesis. The minuscule represents the sequence of T7 promoter.

Results

Characteristics analyses of CmdsRNase2

The ORF of *CmdsRNase2* is 1,335 bp in length, encoding 444 amino acids (Fig. 1A). This zymoprotein contains a signal peptide composed of 16 amino acid residues at the N-terminus, with a molecular weight of 50.55 kDa and a theoretical pI of 8.21. CmdsRNase2 includes 39 negatively charged amino acid residues (D + E) and 42 positively charged amino acid residues (R + K). The aliphatic index and the grand average of hydropathicity (GRAVY) were computed to be 80.81 and − 0.23, respectively. The mature CmdsRNase2 has a domain architecture of DNA/RNA non-specific endonuclease (Endounuclease_NS or NUC) (Fig. 1B), which contains six active sites consisted of one Mg^{2+} binding site, three substrate binding sites, and two catalytic residues. CmdsRNases2 possesses two N-glycosylation sites (N52 and N117), seven O-glycosylation sites, and 42 phosphorylation sites. Multiple sequence alignment of dsRNases from six insects showed evolutionarily conserved amino acids and active sites (Figs. 2 and 3B). The mature CmdsRNase2 (157–390) formed a homodimer with a total of 14 α-helices, 18 β-pleated sheets, and 33 random coils (Fig. 3A). As shown in Fig. 3C, evolutionarily conserved amino acids and their positions are displayed in dark red, and they are vitally important for the structure and function of CmdsRNase2.

Homology comparison and cluster dendrogram

CmdsRNase2 showed 73.74% and 66.44% similarity with CmdsRNase5 and CmdsRNase1 from *C. medinalis*, respectively, 66.96% similarity with *Ostrinia nubilalis* double-stranded ribonuclease 2, and 66.90% and 61.07% similarity with DNA/RNA non-specific endonucleases from *Chilo suppressalis* and *Spodoptera litura*, respectively, based on a Blastp search against the NCBI NR database. Phylogenetic analysis indicated that 16 dsRNases from 12 lepidopteran insects formed two groups and dsRNses from the same family clustered together. Six dsRNases from Pyralidae formed a branch, which clustered with two endonucleases G (EndoGs) from Papilionidae and two dsRNases from Arctiidae into a clade. Six dsRNases from Noctuidae clustered into another clade. For different species, CmdsRNase2 and homolog from *O. nubilalis* gathered together, indicating the closest relationship between them (Fig. 4).

Spatiotemporal expression profile

The ddPCR results showed that the *CmdsRNase2* gene was differentially expressed at various developmental stages of *C. medinalis*, with the highest expression level in the fifth-instar larvae, followed by the fourth-instar larvae, and the lowest level in the pupa. This gene was expressed in the egg, pupa, and adult at relatively low levels; there were no significant differences in expression levels among them. In addition, there was no significant difference in the expression of *CmdsRNase2* between the second- and third-instar larvae (Fig. 5A). The *CmdsRNase2* expression level in the fifth-instar larvae was separately 1.70 times that in the fourth-instar larvae and 33.79 times that in the adult. Among the seven tissues tested, *CmdsRNase2* was expressed at the highest level in the hemolymph, followed by the midgut, and at the lowest level in the integument. This gene was expressed at relatively low levels in the head, integument, fat body, testis, and ovary without significant differences in expression levels among them. The expression level of *CmdsRNase2* in the hemolymph was separately 1.47 times that in the midgut and 4.71 times that in the ovary (Fig. 5B).

A

```
1       ATGCGTTGTTTGGTGATATGGGCTGCAATGGTCCTGGCAGTAACTGCTCATCCTACAATGCCCGATCCATCTGATATG
  1      M  R  C  L  V  I  W  A  A  M  V  L  A  V  T  A  H  P  T  M  P  D  P  S  D  M
79      GTGTTTCTGCTCGATGAAGATGACTTCGAGGATTATCTGGATACCTGGCTGGTTAATGAAGAACAAAGCTGGGTCAAC
 27      V  F  L  L  D  E  D  D  F  E  D  Y  L  D  T  W  L  V  N  E  E  Q  S  W  V  N
157     ATCACGCTAGCCGAGCAAGAGAGAAATGCCGGTGGTTGCATATTCAGAATAAAGGGCGATCTTGGGCAGCCTCAGCCA
 53      I  T  L  A  E  Q  E  R  N  A  G  G  C  I  F  R  I  K  G  D  L  G  Q  P  Q  P
235     GTCTACATCCACAAGAGCAAGCTGTTGATGCCCGCGGGGAACAGCGGGCAGATCCAAGTGAACACTGGCCAGCAGATC
 79      V  Y  I  H  K  S  K  L  L  M  P  A  G  N  S  G  Q  I  Q  V  N  T  G  Q  Q  I
313     GGTTTCGGGTGCACTGGCCGCTACATCCGTCATCCCAACATTACCACCACCACGAATTATGCTACTGCGACATGTGTT
 105     G  F  G  C  T  G  R  Y  I  R  H  P  N  I  T  T  T  T  N  Y  A  T  A  T  C  V
391     CGCGATAACATCGTCTCTGGTAACGGATGGTTACAGGGACAGACTACCTTTGACGAGCTGACTTGTTCGGGCGATGTC
 131     R  D  N  I  V  S  G  N  G  W  L  Q  G  Q  T  T  F  D  E  L  T  C  S  G  D  V
469     TACTTTGAAGCTCAGGCTACTGGTGGCTTATGTTCCGGACTGAATATTGTTATCCGGGCCGGTTACATAGTTGACAAC
 157     Y  F  E  A  Q  A  T  G  G  L  C  S  G  L  N  I  V  I  R  A  G  Y  I  V  D  N
547     GTTTTCCATACCTGGTACCGTTCGTGCTTCAACACAATCCGTTTGGAAGTATTGTACGTGTGGTACGAGCAGACCGCC
 183     V  F  H  T  W  Y  R  S  C  F  N  T  I  R  L  E  V  L  Y  V  W  Y  E  Q  T  A
625     CAACATAGTATCCACGAGGCGAATGTTGTTCGACCCGGTTGGTTAGCTGGTTCCTTCTTTCCGGGTGTGAACATCAAT
 209     Q  H  S  I  H  E  A  N  V  V  R  P  G  W  L  A  G  S  F  F  P  G  V  N  I  N
703     AATGTCTACACGCAAAAAAGCCAAAAGTCAGTGATTGCCGAAATCGTTGGTGATGAAATGGCGAAAACTTACATCACC
 235     N  V  Y  T  Q  K  S  Q  K  S  V  I  A  E  I  V  G  D  E  M  A  K  T  Y  I  T
781     ACTCGACAGTACCTGGTGCGAGGACATCTATCCGCCAAAGTCGACTTCCCGTTTGCGACTGCGCAGCGTTCCACCTTC
 261     T  R  Q  Y  L  V  R  G  H  L  S  A  K  V  D  F  P  F  A  T  A  Q  R  S  T  F
859     TACTTCATCAATGCCGCCCCCCAGTGGTCTCCCTTCAATGGTGGAAACTGGAATAGTCTTGAGCAGTACCTGCGCAAG
 287     Y  F  I  N  A  A  P  Q  W  S  P  F  N  G  G  N  W  N  S  L  E  Q  Y  L  R  K
937     CGCATCGCCGAGGCTGGCTACAACACGGTCATCTACACGGGAACATTCGGGGTGACCCAACTCCGCGACGACAGGAAC
 313     R  I  A  E  A  G  Y  N  T  V  I  Y  T  G  T  F  G  V  T  Q  L  R  D  D  R  N
1015    CGTCTCCGGGATATTTACTTACACAAAACTGGAATTATTCGACAAGTTCCTGTACCTATGTACTTCTATAAGGTGGCT
 339     R  L  R  D  I  Y  L  H  K  T  G  I  I  R  Q  V  P  V  P  M  Y  F  Y  K  V  A
1093    TACGACGAGAGTCGTCGTCTGGGAACGGCTTTCATCAGCATCAACAACCCTTACTACTCGGCGGCTGAGTTGCGCGCC
 365     Y  D  E  S  R  R  L  G  T  A  F  I  S  I  N  N  P  Y  Y  S  A  A  E  L  R  A
1171    CTGCAGTTCTGCACGGACCGCTGCCGCAACAACAGCGCCTTCAGCTGGCTGCGCTGGCAGCCCGACCGCGTCGACCTC
 391     L  Q  F  C  T  D  R  C  R  N  N  S  A  F  S  W  L  R  W  Q  P  D  R  V  D  L
1249    GGCTACAGCTTCTGCTGCACCATCGCCGACTTCAGGAAGAAAATATCTCATATACCCAAATGGAAAGTTAATGGCCTT
 417     G  Y  S  F  C  C  T  I  A  D  F  R  K  K  I  S  H  I  P  K  W  K  V  N  G  L
1327    CTGACATAA
 443     L  T  *
```

B

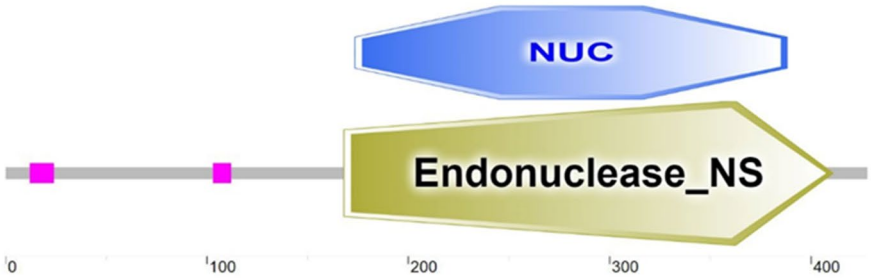

Fig. 1. Nucleotide and deduced amino acid sequences of *CmdsRNase2* (GenBank accession number: OQ938270) (**A**), and domain structure of this mature protein (**B**). The signal peptide is marked in red and the asterisk denotes the stop codon. N- and O-glycosylation sites was marked in blue and green, respectively. In the lower diagram, Endonuclease_NS (168–411) and NUC (169–384) domains denote DNA/RNA non-specific endonuclease, and these two red boxes denote low complexity regions (12–24 and 103–112).

RNAi effect

The expression level of ds*CmRNase2* in the ds*CmRNase2*-injected group decreased by 4.78 and 11.47 times on days 3 and 4 after injection, respectively, compared with the control. On the third day, the *CmCHS* expression reduced by 2.31 and 6.03 times in larvae co-injected with ds*CmCHS* and ds*CmdsRNase2*+ ds*CmCHS*, respectively, as against the control; its expression level in larvae co-injected with ds*CmdsRNase2*+ ds*CmCHS* reduced by 2.61 times compared with that in larvae injected only with ds*CmCHS* (Fig. 6). On day 3 post co-injection of ds*CmdsRNase2*+ ds*CmCHS*, RNAi efficiencies of *CmCHS* and *CmdsRNase2* reached maximums of 83.44% and 53.39%, respectively (Fig. 7A). Therefore, the RNAi efficiency of *CmCHS* in *C. medinalis* was significantly improved by simultaneously interfering with expressions of both *CmCHS* and *CmdsRNase2*.

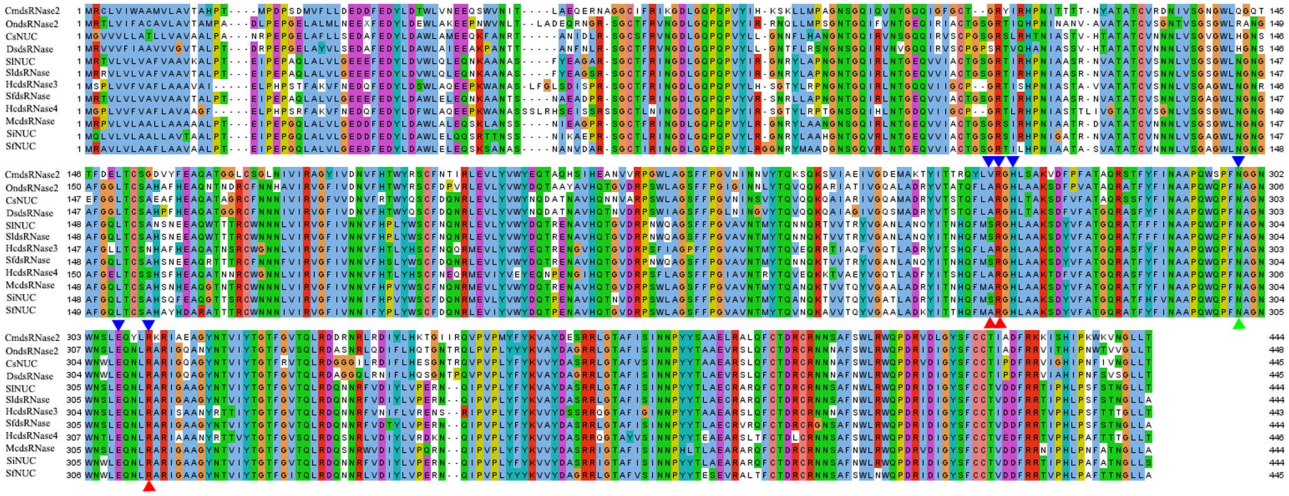

Fig. 2. Multiple sequence alignment of CmdsRNase2 and its homologs from 10 lepidopteran insects. Blue triangles denote six active sites, the green triangle denotes the Mg^{2+} binding site, and red triangles denote three substrate-binding sites. Species and GenBank accession number are the same as those in Fig. 4.

The survival rate of ds*CmCHS*-injected larvae (46.67%) was 1.96 times lower than that of ds*GFP*-injected larvae (91.67%) on day 7 post injection. The percent survival of larvae co-injected with both ds*CmdsRNase2* and ds*CmCHS* (33.33%) was 1.40 times lower than that of larvae injected with ds*CmCHS* alone (46.67%), and 1.45 times lower than that of larvae injected with ds*CmdsRNase2* alone (48.33%) on day 7 (Fig. 7B). In contrast, the injection of ds*GFP* had little effect on larval survival.

Phenotypic changes of the larvae were recorded every day after injection of dsRNA. Larvae in the control had no obvious abnormality in appearance and grew normally (Fig. 8A). However, larvae injected with ds*CmCHS* were significantly affected in the growth and development, such as slow activity, smaller body, yellowed and blackened body, stunted growth, and deformity (Fig. 8B). Larvae co-injected with both ds*CmdsRNase2* and ds*CmCHS* turned black, became smaller in size than those injected with ds*CmCHS* or ds*GFP* (Fig. 8C), and presented with aberrant morphology, for instance, a swollen abdomen and a curled tail. The survival larvae post RNAi could pupate; however, 90% of these pupae turned black in body color and presented with malformed phenotypes (Fig. 8D-F), and eventually died during the pupal development stage. These findings indicated that the co-injection of both ds*CmdsRNase2* and ds*CmCHS* caused not only the developmental arrest of larvae and pupae but also lethal effects.

Discussion

Endogenous dsRNases exist in many insects and one or more dsRNases have been identified in some insects, for example, *Zeugodacus cucurbitae*[31], *Nylanderia fulva*[32], and *Spodoptera frugiperda*[33]. Furthermore, the number of dsRNases involved in dsRNA degradation varies among different insects according to functional studies. Four dsRNase genes were identified from the Asian corn borer *Ostrinia furnacalis*, but OfdsRNase2 contributed to low RNAi efficiency through degrading dsRNA in larvae[20]. Two dsRNase genes were identified and characterized from the midgut of *Locusta migratoria*; however, only LmdsRNase2 was responsible for dsRNA degradation in nymphs[14]. In *S. gregaria*, interference with dsRNase2 improves the RNAi efficiency of dsRNA, while other dsRNases have no effect[34]. Five dsRNase genes were found in *S. litura* and four out of the five dsRNases could degrade dsRNA[9]. In *Plutella xylostella*, four dsRNases were identified and three of the four dsRNases were certified to be involved in the dsRNA degradation to reduce the RNAi efficiency[35]. In *C. puncticollis*, only dsRNase3 can affect its RNAi efficiency[36]; however, in *S. litura*, the combined action of multiple dsRNases leads to a decrease in RNAi efficiency[37], indicating that the number and mechanism of dsRNase actions may be different in different insects. These results suggest that multiple dsRNases function together in RNAi-recalcitrant insects. In *C. medinalis*, six dsRNases were found in the transcriptome of *C. medinalis* but not fully identified, and it is not clear whether all these six enzymes are involved in the dsRNA degradation. Their functions need to be further investigated.

Generally, dsRNases are mainly expressed in the midgut and hemolymph in most insects. However, dsRNase expression is inconsistent in tissues of different insects. DsRNases were mainly expressed in the head and intestine in *T. castaneum*[38], and in the salivary gland and gut in *H. halys*[39]. It was reported that LmdsRNase1 in *L. migratoria* could efficiently degrade dsRNA at pH 5.0 and was highly expressed in the hemolymph, but its activity was suppressed at the physiological pH 7.0 of hemolymph, making dsRNA stably exist in this tissue. In the midgut, LmdsRNase2 digested dsRNA over a broad range of pH 6.0–10[40]. A biochemical comparison of dsRNases in four insects (*S. litura*, *L. migratoria*, *Periplaneta americana*, and *Zophobas atratus*) revealed that these enzymes exhibited high activity in alkaline environments at optimal Mg^{2+} concentrations and elevated temperatures. Additionally, the enzyme activity in their guts was hundreds of times higher than that in other tissues (the whole body, hemolymph, and carcass)[41]. Although dsRNase can be expressed in different tissues,

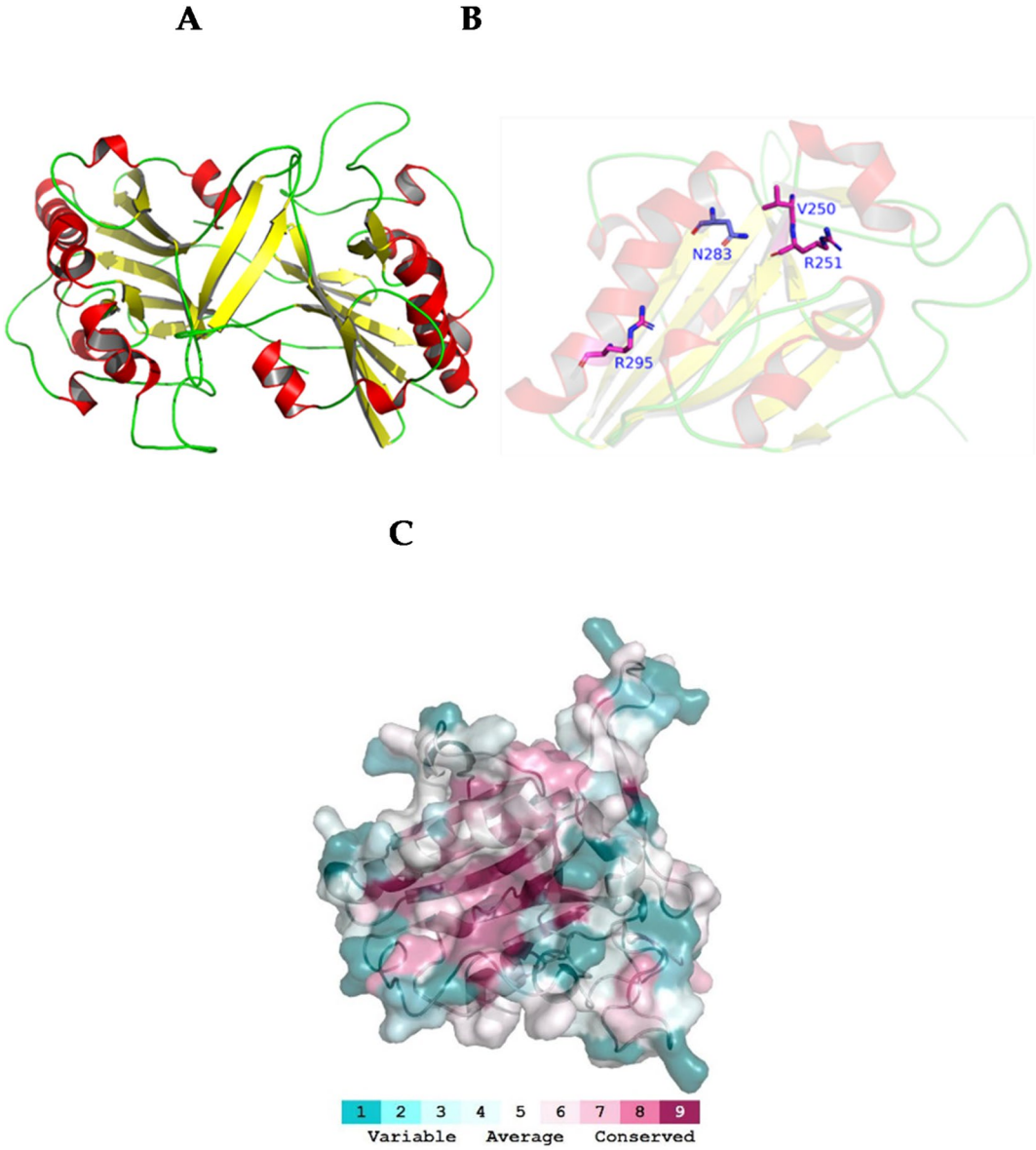

Fig. 3. Three-dimensional molecular structure and evolutionary conservation profile of the mature CmdsRNase2. (**A**) CmdsRNase forming a homodimer. This image was drawn by using PyMOL 3.0 (https://pymol.org), based on the PDB file predicted in SWISS-MODEL (https://swissmodel.expasy.org) with the amino acid sequence of CmdsRNase2. Red represents α-helices, yellow indicates β-pleated sheets, and green denotes random coils. (**B**) A Mg^{2+} binding site (N283) and three substrate binding sites consisting of V250, R251, and R295 in this zymoprotein. This image was drawn with PyMOL 3.0. (**C**) Evolutionary conservation profile of CmdsRNase2. This image was generated with PyMOL 3.0 based on the PDB file predicted in ConSurf (https://consurf.tau.ac.il/consurf_index.php).

due to some factors such as physiological pH or substrate specificity, some enzymes may not degrade dsRNA[19]. A study by Shu et al.. identified six *dsRNase* genes in *Papilio xuthus* and analyzed their expression patterns. The results showed that *PxdsRNase2*, *3*, *5*, and *6* exhibited high expression in the fifth-instar larvae, whereas *PxdsRNase1*, *3*, and *6* were predominantly expressed in the hemolymph, and *PxdsRNase2* was highly expressed in the gut[42]. *CmdsRNase2* is expressed in the fifth-instar larvae with the highest level through developmental stages of *C. medinalis*, probably because the larvae have large food intake and strong vitality, and thus need to express more dsRNases to degrade exogenous dsRNAs. Expression levels of *CmdsRNase2* in the hemolymph and midgut are higher than those in other tissues tested in *C. medinalis* adults, which is consistent with the results in dsRNases expression in other insect tissues[42], and dsRNAs are mainly degraded in these two tissues.

The length of dsRNA could affect dsRNase's activity[43]. It is necessary to study the effect of pH and dsRNA length on the activity of CmdsRNase2 in order to understand the stability of dsRNA in *C. medinalis*. This experiment was only a preliminary study on the degradation of dsRNAs by this enzyme alone. It does not rule out the existence of a synergistic effect between this enzyme and other dsRNases in *C. medinalis*. Therefore, in

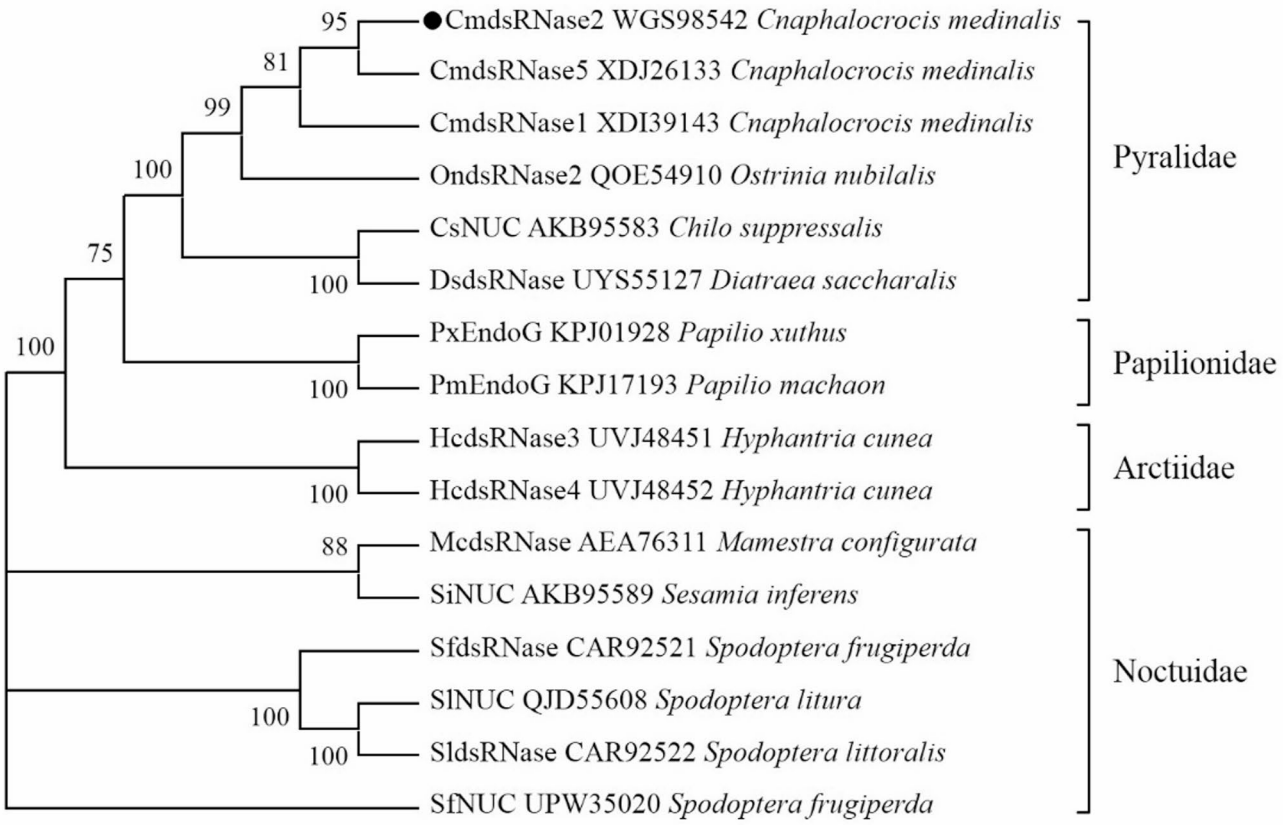

Fig. 4. Phylogenetic tree of dsRNase2 and its homologs from 12 lepidopteran insects. This tree was constructed by using MEGA 11 method with 1,000 repeated runs, based on the neighbor-joining (NJ) method. CmdsRNase2 from *C. medinalis* is marked with the black circle and bootstrap values are showed at nodes.

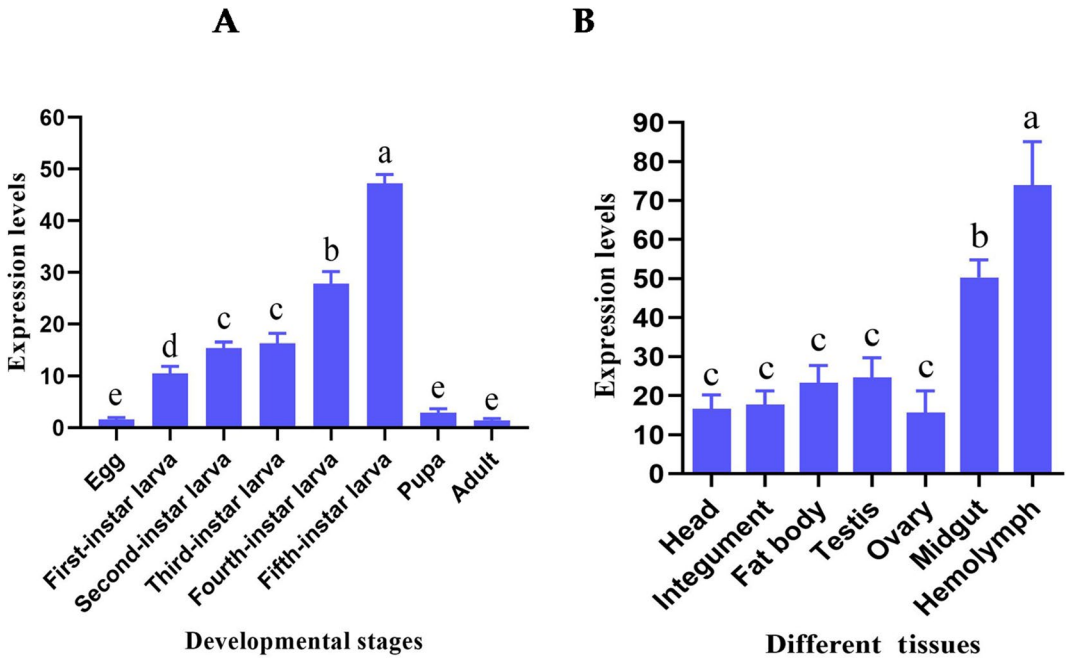

Fig. 5. Expression patterns of *CmdsRNase2* in *C. medinalis*. (**A**) Absolute expression levels (copy/μl) at different developmental stages. (**B**) Absolute expression levels (copy/μl) in different tissues of aduts. Each bar represents the mean ± SD. Different letters above the bars indicate significant differences at $p < 0.05$ based on Duncan's test.

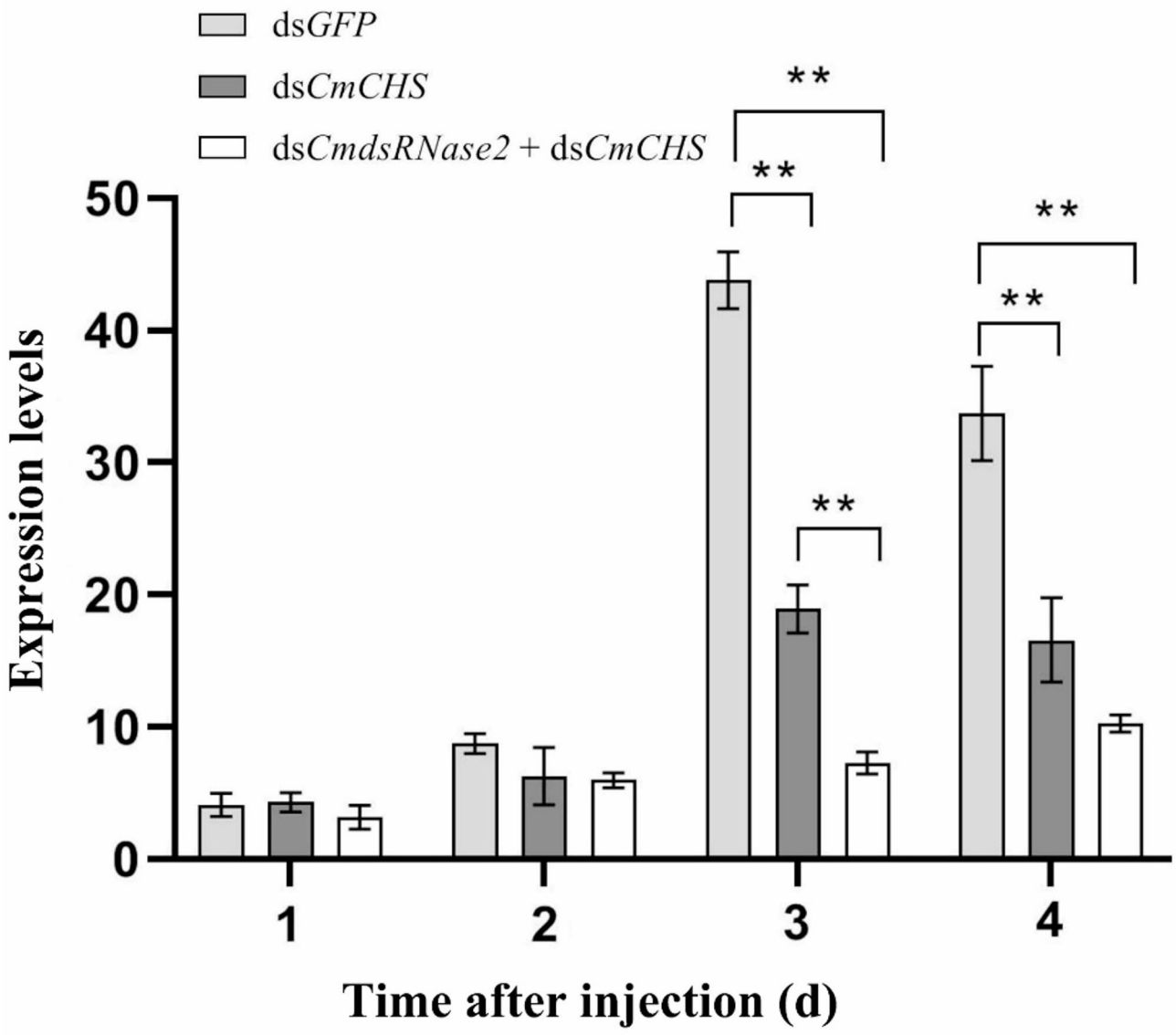

Fig. 6. Expression levels of *CmCHS* at different days after injection of dsRNA. Expression levels of *CmCHS* in *C. medinalis* larvae injected with 1.5 μg of ds*GFP*, a mixture of ds*CmdsRNase2* and ds*CmCHS*, and ds*CmCHS*. Each bar represents the mean ± SD. *, $p < 0.05$; **, $p < 0.01$.

the next step, we will simultaneously silence multiple dsRNases to enhance the RNAi efficacy in rice leaffolder. In addition to silencing *dsRNase* genes via RNAi, knocking out these enzyme genes using gene editing technologies can substantially enhance RNAi efficiency. Koo et al. identified three *dsRNase* genes highly expressed in the midgut of *S. frugiperda* and obtained a homozygous line with knockout of three *dsRNase* genes using CRISPR-Cas9 method. The results suggested that knockout of *dsRNases* might improve RNAi efficiency[44]. Some new techniques such as nanoparticles[45,46], transfection reagents[47], and dsRNA encapsulation are currently under the investigation by many groups for using RNAi technology as a new method for green pest control[48,49]. By combining technologies of dsRNases silencing and lipid nanoparticles for dsRNA delivery to improve RNAi efficiency, RNAi-based green pest control holds great promise in rice leaffolder and other insect pests.

Conclusions

In this paper, the *CmdsRNase2* gene was cloned and characterized from *C. medinalis*. Knockdown of *CmdsRNase2* can enhance the RNAi efficacy of the *CmCHS* gene in rice leaffolder. The simultaneous silencing of both *CmdsRNase2* and a target gene such as *CmCHS* can greatly improve the efficiency of RNAi in *C. medinalis*. This study is very helpful for understanding the mechanism of dsRNase affecting the RNAi efficiency and for environmentally friendly pest control by using RNAi strategies.

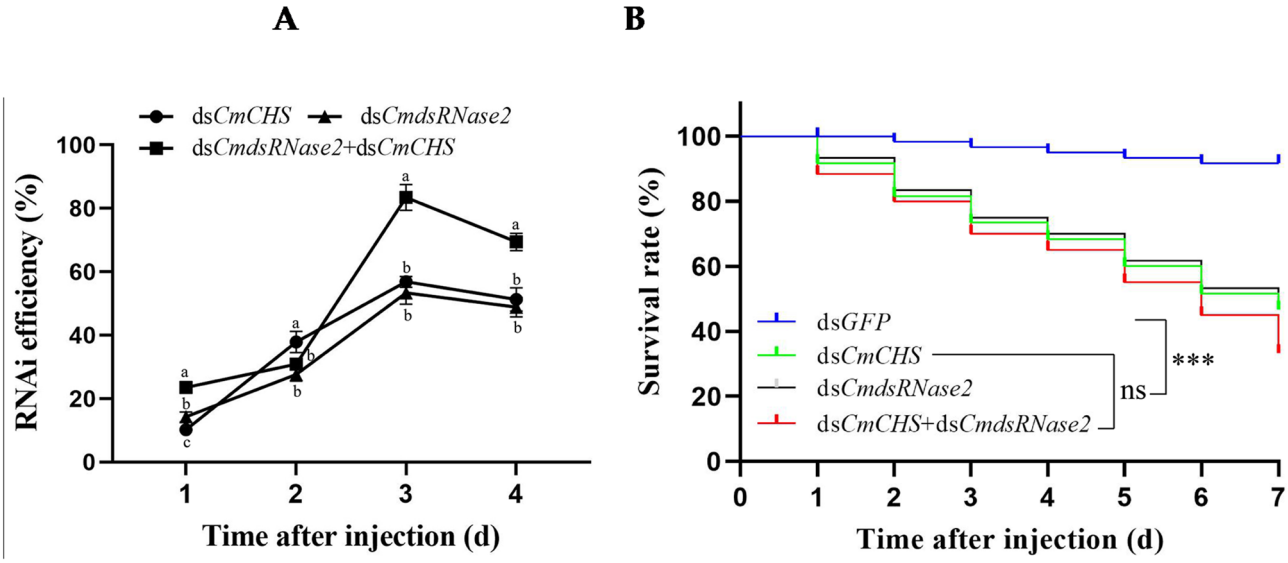

Fig. 7. RNAi efficiency and survival rate at different times. (**A**) RNAi efficiency within 4 d after injection of dsRNA. Data are expressed as means ± SD. Different letters on this line chart indicate significant differences at $p < 0.05$ on the same day based on Duncan's test. (**B**) Survival rate of larvae within 7 d after injection of dsRNA. Asterisks indicate significant differences based on Log-rank test (***, $p < 0.001$) and ns means no significance.

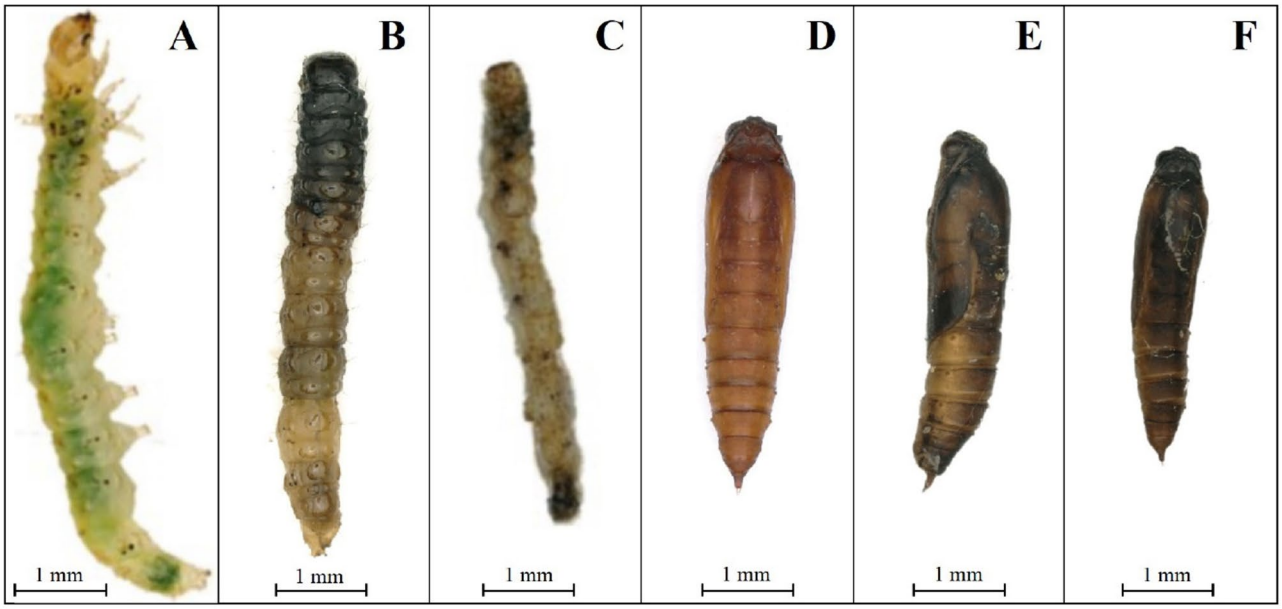

Fig. 8. Aberrant morphology of *C. medinalis* larvae and pupae after injection of dsRNA. (**A**) Phenotypes of larvae injected with ds*GFP*; (**B**) Larvae injected with ds*CmCHS*; (**C**) Larvae co-injected with both ds*CmdsRNase2* and ds*CmCHS*; (**D**) Pupae from larvae of the control; (**E**) Pupae after *CmCHS* RNAi; (**F**) Pupae after both *CmdsRNase2* and *CmCHS* RNAi. Each scale bar represents 1 mm.

Data availability

The datasets generated and analyzed during the current study are available in the GenBank accession number: OQ938270, in the National Center for Biotechnology Information (NCBI).

Received: 6 August 2024; Accepted: 2 May 2025
Published online: 29 May 2025

References

1. Fire, A. et al. Potent and specific genetic interference by double-stranded RNA in *Caenorhabditis elegans*. *Nature* **391**, 806–811. https://doi.org/10.1038/35888 (1998).
2. Terenius, O. et al. RNA interference in lepidoptera: an overview of successful and unsuccessful studies and implications for experimental design. *J. Insect Physiol.* **57**, 231–245. https://doi.org/10.1016/j.jinsphys.2010.11.006 (2011).
3. Joga, M. R., Zotti, M. J., Smagghe, G. & Christiaens, O. RNAi efficiency, systemic properties, and novel delivery methods for pest insect control: What we know so far. *Front. Physiol.* **7**, https://doi.org/10.3389/fphys.2016.00553 (2016).
4. Li, H. et al. Long DsRNA but not SiRNA initiates RNAi in Western corn rootworm larvae and adults. *J. Appl. Entomol.* **139**, 432–445. https://doi.org/10.1111/jen.12224 (2015).
5. Scott, J. G. et al. Towards the elements of successful insect RNAi. *J. Insect Physiol.* **59**, 1212–1221. https://doi.org/10.1016/j.jinsphys.2013.08.014 (2013).
6. Cooper, A. M. W., Silver, K., Zhang, J., Park, Y. & Zhu, K. Y. Molecular mechanisms influencing efficiency of RNA interference in insects. *Pest Manag Sci.* **75**, 18–28. https://doi.org/10.1002/ps.5126 (2019).
7. Cooper, A. M. W. et al. Molecular characterizations of double-stranded RNA degrading nuclease genes from Ostrinia nubilalis. *Insects* **11**, https://doi.org/10.3390/insects11100652 (2020).
8. Miller, M. D., Tanner, J., Alpaugh, M., Benedik, M. J. & Krause, K. L. 2.1-Angstrom structure of *Serratia* endonuclease suggests a mechanism for binding to double-stranded DNA. *Nat. Struct. Biol.* **1**, 461–468. https://doi.org/10.1038/nsb0794-461 (1994).
9. Peng, Y. et al. Identification and characterization of multiple DsRNases from a lepidopteran insect, the tobacco cutworm, *Spodoptera litura* (Lepidoptera: Noctuidae). *Pestic Biochem. Physiol.* **162**, 86–95. https://doi.org/10.1016/j.pestbp.2019.09.011 (2020).
10. Friedhoff, P., Gimadutdinow, O. & Pingoud, A. Identification of catalytically relevant amino acids of the extracellular *Serratia marcescens* endonuclease by alignment-guided mutagenesis. *Nucleic Acids Res.* **22**, 3280–3287. https://doi.org/10.1093/nar/22.16.3280 (1994).
11. Gregor, M. & Frank, U. G. The DNA/RNA non-specific *Serratia* nuclease prefers double-stranded A-form nucleic acids as substrates. *J. Mol. Biology*. **288**, 377–390. https://doi.org/10.1006/jmbi.1999.2694 (1999).
12. Loll, B., Gebhardt, M., Wahle, E. & Meinhart, A. Crystal structure of the endog/endogi complex: mechanism of endog Inhibition. *Nucleic Acids Res.* **37**, 7312–7320. https://doi.org/10.1093/nar/gkp770 (2009).
13. Arimatsu, Y., Kotani, E., Sugimura, Y. & Furusawa, T. Molecular characterization of a cDNA encoding extracellular DsRNase and its expression in the silkworm, *Bombyx mori*. *Insect Biochem. Mol. Biol.* **37**, 176–183. https://doi.org/10.1016/j.ibmb.2006.11.004 (2007).
14. Song, H. et al. A double-stranded RNA degrading enzyme reduces the efficiency of oral RNA interference in migratory locust. *Insect Biochem. Mol. Biol.* **86**, 68–80. https://doi.org/10.1016/j.ibmb.2017.05.008 (2017).
15. Mukai, J. I. An endonuclease from silkworm—purification and mode of action. *Biochem. Biophys. Res. Commun.* **21**, 562–567. https://doi.org/10.1016/0006-291x(65)90522-x (1965).
16. Meegan, J. M. & Marcus, P. I. Double-stranded ribonuclease coinduced with interferon. *Science* **244**, 1089–1091. https://doi.org/10.1126/science.2471268 (1989).
17. Marcus, P. I. & Yoshida, I. Mycoplasmas produce double-stranded ribonuclease. *J. Cell. Physiol.* **143**, 416–419. https://doi.org/10.1002/jcp.1041430303 (1990).
18. Liu, J., Swevers, L., Iatrou, K., Huvenne, H. & Smagghe, G. *Bombyx mori* DNA/RNA non-specific nuclease: expression of isoforms in insect culture cells, subcellular localization and functional assays. *J. Insect Physiol.* **58**, 1166–1176. https://doi.org/10.1016/j.jinsphys.2012.05.016 (2012).
19. Wynant, N. et al. Identification, functional characterization and phylogenetic analysis of double stranded RNA degrading enzymes present in the gut of the desert locust, *Schistocerca gregaria*. *Insect Biochem. Mol. Biol.* **46**, 1–8. https://doi.org/10.1016/j.ibmb.2013.12.008 (2014).
20. Fan, Y. H. et al. A dsRNA-degrading nuclease (dsRNase2) limits RNAi efficiency in the Asian corn borer (*Ostrinia furnacalis*). *Insect Sci.* **28**, 1677–1689. https://doi.org/10.1111/1744-7917.12882 (2021).
21. Peng, Y. et al. Knockout of *SldsRNase1* and *SldsRNase2* revealed their function in DsRNA degradation and contribution to RNAi efficiency in the tobacco cutworm, *Spodoptera litura*. *J. Pest Sci.* **94**, 1449–1460. https://doi.org/10.1007/s10340-021-01335-w (2021).
22. Zhang, X. et al. RNAi efficiency through DsRNA injection is enhanced by knockdown of DsRNA nucleases in the fall webworm, *Hyphantria cunea* (Lepidoptera: Arctiidae). *Int. J. Mol. Sci.* **23**, 6182. https://doi.org/10.3390/ijms23116182 (2022).
23. Chen, P., Dai, C., Liu, H. & Hou, M. Identification of key headspace volatile compounds signaling preference for rice over corn in adult females of the rice leaf folder *Cnaphalocrocis Medinalis*. *J. Agric. Food Chem.* **70**, 9826–9833. https://doi.org/10.1021/acs.jafc.2c01948 (2022).
24. Liao, H. J., Huang, J. R. & Liu, X. D. The method for mass rearing of rice leaf folder *Cnaphalocrocis Medinalis* using maize seedlings. *Chin. J. Appl. Entomol.* **49**, 1078–1082 (2012).
25. Murthy, M. S., Nagaraj, S. K., Prabhuraj, A. & Kalleswaraswamy, C. M. Rice leaf folder *Cnaphalocrocis Medinalis* (Lepidoptera: Crambidae) on wheat (*Triticum aestivum*; Poales: Poaceae) in India. *Fla. Entomol.* **98**, 1269–1270 (2015).
26. Riley, J. R. et al. Observations of the autumn migration of the rice leaf roller *Cnaphalocrocis Medinalis* (Lepidoptera: Pyralidae) and other moths in Eastern China. *B Entomol. Res.* **85**, 397–414 (1995).
27. Sun, Y. et al. Insecticide resistance monitoring of *Cnaphalocrocis Medinalis* (Lepidoptera: Pyralidae) and its mechanism to Chlorantraniliprole. *Pest Manag Sci.* **79**, 3290–3299. https://doi.org/10.1002/ps.7512 (2023).
28. Yang, Y., Wang, C., Xu, H. & Lu, Z. Sublethal effects of four insecticides on folding and spinning behavior in the rice leaffolder, *Cnaphalocrocis Medinalis* (Guenee) (Lepidoptera: Pyralidae). *Pest Manag Sci.* **74**, 658–664. https://doi.org/10.1002/ps.4753 (2018).
29. Li, J., Du, J., Li, S. & Wang, X. Identification and characterization of a double-stranded RNA degrading nuclease influencing RNAi efficiency in the rice leaf folder *Cnaphalocrocis Medinalis*. *Int. J. Mol. Sci.* **23**, 3961. https://doi.org/10.3390/ijms23073961 (2022).
30. Mo, M. et al. Identification and functional analyses of the *CmdsRNase5* and *CmdsRNase6* genes in rice leaffolder *Cnaphalocrocis Medinalis*. *Int. J. Biol. Macromol.* **301**, 140079. https://doi.org/10.1016/j.ijbiomac.2025.140079 (2025).
31. Ahmad, S., Jamil, M., Jaworski, C. C. & Luo, Y. Double-stranded RNA degrading nuclease affects RNAi efficiency in the melon fly, *Zeugodacus cucurbitae*. *J. Pest Sci.* **97**, 397–409. https://doi.org/10.1007/s10340-023-01637-1 (2024).
32. Lei, J. et al. Cloning and functional characterization of a double-stranded RNA-degrading nuclease in the Tawny crazy ant (*Nylanderia fulva*). *Front. Physiol.* **13**, 833652. https://doi.org/10.3389/fphys.2022.833652 (2022).
33. Yao, Y. et al. Multiple DsRNases involved in exogenous DsRNA degradation of fall armyworm *Spodoptera frugiperda*. *Front. Physiol.* **13**, 850022. https://doi.org/10.3389/fphys.2022.850022 (2022).
34. Spit, J. et al. Knockdown of nuclease activity in the gut enhances RNAi efficiency in the Colorado potato beetle, Leptinotarsa decemlineata, but not in the desert locust, *Schistocerca gregaria*. *Insect Biochem. Mol. Biol.* **81**, 103–116. https://doi.org/10.1016/j.ibmb.2017.01.004 (2017).
35. Chen, J. Z. et al. Double-stranded RNA-degrading enzymes reduce the efficiency of RNA interference in *Plutella Xylostella*. *Insects* **12**, 712. https://doi.org/10.3390/insects12080712 (2021).
36. Prentice, K., Smagghe, G., Gheysen, G. & Christians, O. Nuclease activity decreases the RNAi response in the Sweetpotato weevil *Cylas puncticollis*. *Insect Biochem. Mol. Biol.* **110**, 80–89. https://doi.org/10.1016/j.ibmb.2019.04.001 (2019).
37. Meiss, G., Gast, F. U. & Pingoud, A. M. The DNA/RNA non-specific *Serratia* nuclease prefers double-stranded *A*-form nucleic acids as substrates. *J. Mol. Biol.* **288**, 377–390. https://doi.org/10.1006/jmbi.1999.2694 (1999).

38. Peng, Y. et al. Identification of a double-stranded RNA-degrading nuclease influencing both ingestion and injection RNA interference efficiency in the red flour beetle *Tribolium castaneum*. *Insect Biochem. Mol. Biol.* **125**, 103440. https://doi.org/10.1016/j.ibmb.2020.103440 (2020).
39. Lomate, P. R. & Bonning, B. C. Proteases and nucleases involved in the biphasic digestion process of the brown marmorated stink bug, *Halyomorpha halys* (Hemiptera: Pentatomidae). *Arch. Insect Biochem. Physiol.* **98**, e21459. https://doi.org/10.1002/arch.21459 (2018).
40. Song, H. et al. Contributions of DsRNases to differential RNAi efficiencies between the injection and oral delivery of DsRNA in *Locusta migratoria*. *Pest Manag Sci.* **75**, 1707–1717. https://doi.org/10.1002/ps.5291 (2019).
41. Peng, Y., Wang, K., Fu, W., Sheng, C. & Han, Z. Biochemical comparison of DsRNA degrading nucleases in four different insects. *Front. Physiol.* **9**, 624. https://doi.org/10.3389/fphys.2018.00624 (2018).
42. Shu, Q. et al. RNAi efficiency is enhanced through knockdown of double-stranded RNA-degrading enzymes in butterfly *Papilio xuthus*. *Arch. Insect Biochem. Physiol.* **115**, e22113. https://doi.org/10.1002/arch.22113 (2024).
43. Wang, K., Peng, Y., Fu, W., Shen, Z. & Han, Z. Key factors determining variations in RNA interference efficacy mediated by different double-stranded RNA lengths in *Tribolium castaneum*. *Insect Mol. Biol.* **28**, 235–245. https://doi.org/10.1111/imb.12546 (2019).
44. Koo, J., Zhu, G. H. & Palli, S. R. CRISPR-Cas9 mediated DsRNase knockout improves RNAi efficiency in the fall armyworm. *Pestic Biochem. Physiol.* **200**, 105839. https://doi.org/10.1016/j.pestbp.2024.105839 (2024).
45. Zhang, X., Zhang, J. & Zhu, K. Y. Chitosan/double-stranded RNA nanoparticle-mediated RNA interference to silence Chitin synthase genes through larval feeding in the African malaria mosquito (*Anopheles gambiae*). *Insect Mol. Biol.* **19**, 683–693. https://doi.org/10.1111/j.1365-2583.2010.01029.x (2010).
46. He, B. C. et al. Fluorescent nanoparticle delivered DsRNA toward genetic control of insect pests. *Adv. Mater.* **25**, 4580–4584. https://doi.org/10.1002/adma.201301201 (2013).
47. Sanitt, P. et al. Cholesterol-based cationic liposome increases DsRNA protection of yellow head virus infection in *Penaeus vannamei*. *J. Biotechnol.* **228**, 95–102. https://doi.org/10.1016/j.jbiotec.2016.04.049 (2016).
48. Yang, J. & Han, Z. J. Efficiency of different methods for DsRNA delivery in cotton bollworm (*Helicoverpa armigera*). *J. Integr. Agr.* **13**, 115–123. https://doi.org/10.1016/S2095-3119(13)60511-0 (2014).
49. Wang, G. et al. Effects of double-stranded RNA degrading nucleases on RNAi efficiency in beet moth *Spodoptera exigua* (Lepidoptera: Noctuidae). *Insects* **16**, 229. https://doi.org/10.3390/insects16020229 (2025).

Acknowledgements

This work was supported by the National Natural Science Foundation of China (Nos. 31360443 and 32060641), and Qiandongnan Science and Technology Plan Project (No. 202307).

Author contributions

S.L. and R.Z. designed the research; X.W., R.Z. and J.L. performed all the experiments; X.W. and J.L. analyzed the data; S.L., X.W., J.L. and J.D. wrote the manuscript. All authors reviewed the manuscript.

Declarations

Competing interests

The authors declare no competing interests.

Additional information

Correspondence and requests for materials should be addressed to S.L. or R.Z.